Conformation Study of Helical Main-Group Polymers: Organic and Inorganic, Trans and Gauche

C. X. Cui[†] and Miklos Kertesz*[,‡]

Contribution from the Department of Chemistry, Georgetown University, Washington, D.C. 20057. *Received November 9, 1988*

Abstract: In this paper electronic structures of some helical polymers, which range from typical organic polymers such as polyethylene and poly(oxymethylene) to standard inorganic polymers such as polymeric sulfur to main-group (P, B, etc.) atomic chains in crystals (such as NaP, CrB, etc.), have been investigated by means of our helical modifications of solid-state band theory programs based on modified neglect of diatomic overlap (MNDO) and extended Hückel theory (EHT). The analysis of orbital interactions shows that the all-trans conformation for the polymer with either less or more than six valence electrons in the repeat unit is energetically favorable as compared with the gauche conformation while the polymers having valence electrons close to six in the repeat unit are more likely to be found in a gauche conformation, except for polyethylene and polysilane, for which both conformations are stable. The stability of *all-trans*-polyethylene and -polysilane is attributed to the weak repulsions between C–H and Si–H bonding electron pairs. A quadratic relationship between band width and the corresponding closed-shell repulsion for an energy band is established.

Many biopolymers, more than half of the known crystal structures of organic polymers, and many inorganic polymers exist in helical conformations.[1,2] Some of them, such as DNA and polyethylene, are of great practical and theoretical interest.[2] Polymeric sulfur also forms helices and often serves to test theories of the spatial configurations of chain molecules in the field of polymer statistics and critical phenomena.[3] Selenium, which forms 3-fold helical chains, is an important semiconducting material and has been studied in detail both experimentally and theoretically for many years.[4] A large number of intermetallic phases incorporate chains of main-group IIIA,[5] IVA,[6] or VA[7] elements in zigzag planar or helical conformations. Among these phases, those containing main-group IV and V elements are usually Zintl phases, while the binary metallic phases of main-group III elements and metal atoms are not following Zintl's rule[8] such as $GaLi_2$, where Ga atoms form zigzag planar chains[5b] as do the Sb atoms in $CaSb_2$.[7e] On the other hand, the Sb atoms form a distorted 4-fold helix in CsSb[7g] similar to the P^- chains in NaP.[7f] What drives some of these structures to form helices? As we show in this paper, in a very broad class of cases the underlying reasons are of electronic nature.

In this paper we will study comparatively various helical polymers whose main-chain atoms have a tetrahedral (sp^3) electron configuration surrounded by four electron pairs, as listed in Table I. Comparison with sp^2 cases will also be made. Related systems, namely, polyacetylene,[10] the Li_2Ga phase, and crystals with NaP[7f] and CrB[5a] structures are investigated and discussed as well.

The relationships of the parameters describing the main chain atoms of these polymers, bond distance (r), bond angle (α) and dihedral angle (τ) on the one hand, and an operation of screw axis of symmetry (rotation by θ, translation by h along the Z axis, and the radius ρ), are illustrated in **1**.

Most of the polymers listed in Table I have been studied theoretically, but no fully optimized geometries (except for sulfur) have been reported using quantum chemical techniques up to now.[11] Table I shows that the experimental bond angles for these polymers are about 110° and dihedral angles, except for polyethylene, are about 80°. However, theoretical calculations have shown that the gauche conformation of polyethylene has a C–C–C–C dihedral angle along the main chain of about 80°.[12] This gauche conformation is not far in energy from the more stable all-trans one, as we will see later.

In this paper we develop connections among quite different helical polymers and crystals. By analyzing the orbital patterns

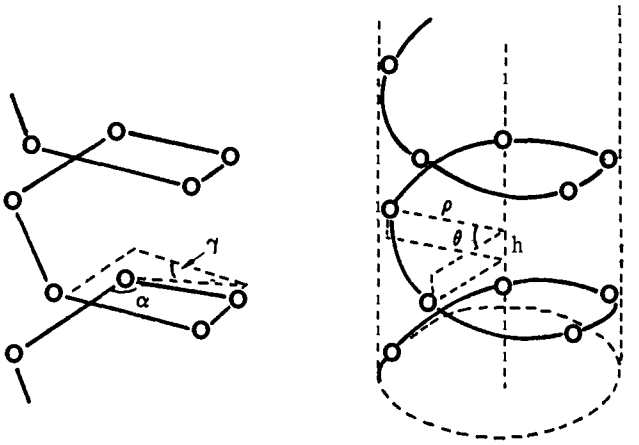

1

of helical chains in various configurations, we show that striking similarities exist among some of these rather different systems,

[†] Permanent address: Institute of Theoretical Chemistry, Jilin University, Changchun, PRC.

[‡] Camille and Henry Dreyfus Teacher-Scholar, 1984–1989.

(1) (a) Wells, A. F. *Structural Inorganic Chemistry*; Clarendon: Oxford University, 1984. (b) Tadokoro, H. *Structure of Crystalline Polymers*; Wiley: New York, 1979.

(2) Walton, A. G.; Blackwell, J. *Biopolymers*; Academic Press: New York, 1973; and ref 10.

(3) (a) Mark, J. E.; Curro, J. G. *J. Chem. Phys.* **1984**, *80*, 5262. (b) Tuinstra, F. *Acta Crystallogr.* **1966**, *20*, 341. (c) Lind, M. D.; Geller, S. *J. Chem. Phys.* **1969**, *51*, 348. (d) Geller, S.; Lind, M. D. *Acta Crystallogr.* **1969**, *B25*, 2166.

(4) (a) Cherin, P.; Unger, P. *Inorg. Chem.* **1967**, *8*, 1589. (b) Gerlach, E.; Grosse, P. *The Physics of Selenium and Tellurium*; Springer Series in Solid State Science, Vol. 13. Springer: Berlin, 1979; (c) Harrison, W. A. *Electronic Structure and the Properties of Solid*; W. H. Freeman: New York, 1980. (d) Burdett, J. K.; Lee, S. *J. Am. Chem. Soc.* **1985**, *107*, 3063. (e) Cui, C. X.; Jiang, Y. *Wuli Huaxue Xuebao* **1987**, *3*, 581.

(5) (a) Kiessling, R. *Acta Chem. Scand.* **1949**, *3*, 595. (b) Muller, W.; Stohr, J. *Z. Naturforsch.* **1977**, *32B*, 631. (c) Bjurstrom, T. *Ark. Kemi, Mineral. Geol.* **1933**, *11A*, 12. (d) Bjurstrom, T. *Z. Physik.* **1929**, *B4*, 469. (e) Kiessling, R. *Acta Chem. Scand.* **1947**, *1*, 893. (f) Kiessling, R. *Acta Chem. Scand.* **1949**, *3*, 90. (g) Kiessling, R. *Acta Chem. Scand.* **1950**, *4*, 209. (h) Decker, B. F.; Kasper, J. S. *Acta Crystallogr.* **1954**, *7*, 77. (i) Rudy, E.; Benesorsky, F. *Monatsch. Chem.* **1961**, *92*, 415. (j) Rudy, E.; Benesorsky, F. *Z. Metallk.* **1963**, *54*, 345. (k) Lundstrom, T. *Ark. Kemi.* **1969**, *31*, 227. (l) Popesch, G.; Nowotny, H.; Benesorsky, F. *Monatsh. Chem.* **1973**, *104*, 933. (m) Rundqvist, S. *Acta Chem. Scand.* **1959**, *13*, 1193.

(6) (a) Heller, E. *Z. Anorg. Chem.* **1950**, *261*, 226. (b) Eckerlin, P.; Meyer, H. J.; Wolfel, E. *Z. Anorg. Chem.* **1955**, *281*, 322. (c) Rocktaschel, R.; Weiss, A. *Z. Anorg. Chem.* **1962**, *316*, 261. (d) Sands, D. E.; Wood, D. H.; Ramsey, W. J. *Acta Crystallogr.* **1964**, *17*, 986. (e) Burnashowa, W. W.; Gladyshevskii, E. I. *Izv. Akad. Nauk SSSR, Neorg. Mater.* **1965**, *2*, 944. (f) Rieger, W.; Parthe, E. *Acta Crystallogr.* **1967**, *22*, 919.

0002-7863/89/1511-4216$01.50/0

Table I. Selected Polymers with Eight Valence Electrons around the Main-Chain Atoms with Their Experimental Structural Data

polym	L,[a] Å	α,[b] deg	τ,[c] deg	θ,[e] deg	ref
$(S)_x$	2.07	106.0	85	108.0	3b
$(Se)_x$	2.373	103.1	101	120.0	4a
$(CH_2)_x$	1.541 (C–C)	112.0 (CCC)	180	180.0	9a
$(CH_2O)_x$	1.429 (C–O)	112.9 (COC)	77	198.6	9b
		110.0 (OCO)	77		
$(CH_2S)_x$			66[f]	190.6	9c

[a] Bond length. [b] Bond angle. [c] Dihedral angle. [e] Helical angle. [f] Deduced value based on assumed standard bond lengths and bond angles.

which however, have the same connectivity and same electron count. We will identify the electronic reasons why polyethylene can exist in all-trans and gauche conformations[13] and only the gauche conformation is found for other polymers listed in Table I. We will also see the effect of changing electron counting on the conformation of helical polymers. For this purpose full geometry optimization for the polymers listed in Table I are performed by our modification of an MNDO (modified neglect of diatomic overlap) solid-state program.[14] The band structures obtained by the modified extended Hückel solid-state program are used for the orbital interpretation of the results.

Calculation Method

The theoretical methods to calculate electronic band structures for polymers within the framework of the Hartree–Fock one-electron approximation have been described and reviewed by different authors based on the assumption that the polymers have translational symmetry.[15-17] However, this approach is applicable only to polymers having a small translational repeat unit. Helical polymers usually have too large translational repeat units to be treated effectively. For example, in elemental sulfur, there are 10 sulfur atoms in the translational unit cell.[3b] Furthermore, when the geometry is optimized at irrational values of the helical angle θ, there is no translational symmetry at all in the system. The best way to reduce the numerical effort and to allow an optimization as a function of helical angle is to consider explicitly the helical symmetry as proposed by Imamura and Fujita,[18] Ukrainskii,[19] and Blumen and Merkel.[20] These authors have shown that the computationally relevant unit to consider is the unit cell which is being repeated by the application of the operation of the screw axis of symmetry. Not only is the size of the secular matrices reduced in this way, but also the number of two-electron integrals to be evaluated diminishes considerably. We have incorporated helical symmetry into an MNDO solid-state program[21] as well as an extended Hückel solid-state program.[22] The reason we choose these two approaches is that the MNDO method produces reasonable optimized geometries for organic polymers without using vast amounts of computer time[14,23] and the extended Hückel method has formed the cornerstone of some illuminating analysis of the factors influencing the geometries of a variety of organic and inorganic molecules and extended systems.[24]

The helical system **1** is invariant under the screw operation $\hat{S}(l,q)$, i.e., a rotation through $2\pi ql$, followed by a translation by a distance of lh along the screw axis (Z), where h is translation per repeat unit and l is an integer. $\theta = 2\pi q$ is the angle of rotation of the screw. When q is a rational number, the helical polymer **1** has translational symmetry in addition to the screw axis of symmetry and cyclic boundary conditions[25] are applicable. If q is an irrational number, the helical system **1** has no translational symmetry at all, merely a screw axis of symmetry. Earlier formulations concerning electronic structure calculations for helical polymers have been derived by using cyclic boundary conditions.[18,19] Blumen and Merkel have pointed out that a pure screw axis can be treated analogously to translations.[20] In fact, it is easy to prove that all symmetry operators $\hat{S}(q,l)$ with either rational or irrational q form an Abelian group that has only one-dimensional representations which are complex roots of unity.[25] The character for $\hat{S}(q,l)$ is $\exp(i\mathbf{k}hl)$, where $\mathbf{k}$ ranges from $-\pi/h$ to π/h and labels the irreducible representation. The projection operators are given by[25]

$$\hat{P}_{\mathbf{k}} = \sum_l \exp(i\mathbf{k}hl)\hat{S}(q,l) \tag{1}$$

Applying $\hat{P}_{\mathbf{k}}$ to any function, it will project out the component of the function which transforms as the irreducible representation $\mathbf{k}$. The symmetry-adapted linear combinations of atomic orbitals for helical polymers, the pseudo-Bloch function, therefore are written as follows:

$$B_p(\mathbf{k}) = \sum_l \exp(i\mathbf{k}hl)\chi^p{}_l \tag{2}$$

where $\chi^p{}_l$ is the pth atomic orbital in the lth repeat unit and is generated by applying $\hat{S}(l,q)$ to the pth atomic orbital located in the reference ($l = 0$) repeat unit. The reason we call B_p a pseudo-Bloch function is that even if B_p belongs to the same $\mathbf{k}$ as a usual Bloch function, they may have a different nodal structure as compared to a Bloch function generated by translational symmetry. For example, in the case of a linear zigzag chain with a 2-fold screw axis, the usual Bloch function consists of the in-phase combinations (**2a**) at $\mathbf{k} = 0.0$ while B_p is an out-of-phase combination of p_x orbital as shown in **2b**.

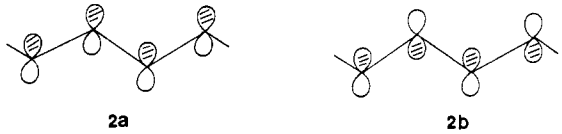

2a **2b**

(7) (a) Cromer, D. T. *Acta Crystallogr.* **1959**, *12*, 36. (b) Cromer, D. T. *Acta Crystallogr.* **1959**, *12*, 41. (c) Busmann, E.; Lohmexer, S. *Z. Anorg. Allg. Chem.* **1961**, *312*, 53. (d) Langer, K.; Juza, R. *Naturwissenschaften* **1967**, *54*, 225. (e) Deller, K.; Eisenmann, B. *Z. Anorg. Allg. Chem.* **1976**, *425*, 104. (f) Schering, H. G. v.; Honle, W. *Z. Anorg. Allg. Chem.* **1979**, *456*, 194. (g) Schering, H. G. v.; Honle, W.; Krogull, G. *Z. Naturforsch.* **1979**, *B34*, 1678.

(8) (a) Zintl, E.; Woltersdorf, G. *Z. Electrochem. Angew. Phys. Chem.* **1935**, *41*, 876. (b) Zintl, E. *Angew. Chem.* **1939**, *52*, 1. (c) Schafer, H.; Eisenmann, B.; Muller, W. *Angew. Chem., Int. Ed. Engl.* **1973**, *12*, 694.

(9) (a) Kavesh, S.; Schultz, J. M. *J. Polym. Sci. Part A* **1970**, *2*, 243. (b) Takahashi, Y.; Tadokoro, H. *J. Polym. Sci., Polym. Phys. Ed.* **1979**, *17*, 123. (c) Carazzolo, G.; Valle, G. *Makromol. Chem.* **1966**, *66*, 90.

(10) Chien, J. C. W. *Polyacetylene*; Academic Press: New York, 1984.

(11) For polyethylene see: (a) McCubbin, W. L.; Manne, R. *Chem. Phys. Lett.* **1968**, *2*, 230. (b) Imamura, A. *J. Chem. Phys.* **1970**, *52*, 3168. (c) McCubbin, W. L. *Chem. Phys. Lett.* **1971**, *8*, 507. (d) Fujita, H.; Imumura, A. *J. Chem. Phys.* **1970**, *53*, 4555. (e) Morokuma, K. *Chem. Phys. Lett.* **1970**, *6*, 186. (f) Morosi, G.; Simonnetta, M. *Chem. Phys. Lett.* **1971**, *8*, 358. (g) O'Shea, S.; Santry, D. P. *J. Chem. Phys.* **1971**, *54*, 2667. (h) Wood, M. H.; Barber, M.; Hiller, I. H.; Thomas, J. M. *J. Chem. Phys.* **1972**, *56*, 1788. (i) Andre, J. M.; Delhalle, J.; Kapsomenos, G.; Leroy, G. *Chem. Phys. Lett.* **1972**, *14*, 485. (j) McAloon, B. J.; Perkins, P. G. *Trans. Faraday Soc.* **1973**, *69*, 1793. (k) Duke, B. J.; O'Leary, B. *Chem. Phys. Lett.* **1973**, *20*, 459. (l) Perkins, P. G.; Marwaha, A. K.; Stewart, J. J. P. *Theor. Chim. Acta* **1980**, *57*, 1. (m) Beveridge, D. L.; Jano, I.; Ladik, J. *J. Chem. Phys.* **1972**, *56*, 4744. (n) Dewar, M. J. S.; Yamaguchi, Y.; Suck, S. H. *Chem. Phys. Lett.* **1977**, *50*, 259. (o) Kasowski, R. V.; Hsu, W. Y.; Caruthers, E. B. *J. Chem. Phys.* **1980**, *72*, 4896. (p) Karpfen, A.; Beyer, A. *J. Comput. Chem.* **1984**, *5*, 11. (q) Karpfen, A. *J. Chem. Phys.* **1981**, *75*, 238. For polymeric sulfur see: (r) Springborg, M.; Jones, R. O. *Phys. Rev. Lett.* **1986**, *57*, 1145. (s) Karpfen, A. *Chem. Phys. Lett.* **1987**, *136*, 571. For poly(oxymethylene) see: (t) Ohsaku, M.; Imamura, A. *Macromolecules* **1978**, *11*, 970. (u) Karpfen, A.; Beyer, A. *J. Comput. Chem.* **1984**, *5*, 19.

(12) Scott, R. A.; Scheraga, H. A. *J. Chem. Phys.* **1966**, *44*, 3054.

(13) Mizushima, M.; Shimanouchi, T. *J. Phys. Chem.* **1952**, *52*, 324.

(14) (a) Dewar, M. J. S.; Thiel, W. *J. Am. Chem. Soc.* **1977**, *99*, 4899, 4907. (b) Stewart, J. J. P. *QCPE Bull.* **1985**, *5*, 62; *MOSOL Manual*; USAF, Colorado, Springs, 1984. (c) Lee, Y.; Kertesz, M. *J. Chem. Phys.* **1988**, *88*, 2609.

(15) (a) Peacock, T. E.; McWeeny, R. *Proc. Phys. Soc., London* **1959**, *74*, 385. (b) Del Re, G.; Ladik, J.; Biczo, G. *Phys. Rev.* **1967**, *155*, 997.

(16) Andrê, J.-M. *Adv. Quantum Chem.* **1980**, *12*, 65.

(17) Kertesz, M. *Adv. Quantum Chem.* **1982**, *15*, 161.

(18) Imamura, A.; Fujita, H. *J. Chem. Phys.* **1974**, *61*, 115.

(19) Ukrainskii, I. I. *Theor. Chim. Acta* **1975**, *38*, 139.

(20) Blumen, A.; Merkel, C. *Phys. Status Solidi* **1977**, *B83*, 425.

(21) Dewar, M. J. S.; Yamaguchi, Y.; Suck, S. H. *Chem. Phys.* **1979**, *43*, 145.

(22) (a) Hoffmann, R. *J. Chem. Phys.* **1963**, *39*, 1397. (b) Whangbo, M.-H.; Hoffmann, R. *J. Am. Chem. Soc.* **1978**, *100*, 6093.

(23) Kertesz, M.; Lee, S. *J. Phys. Chem.* **1987**, *91*, 2690.

(24) For a review see: Albright, T. A.; Burdett, J. K.; Whangbo, M. H. *Orbital Interactions in Chemistry*; Wiley: New York, 1985.

(25) Lax, M. *Symmetry Principles in Solid State and Molecular Physics*; Wiley: New York, 1974.

Table II. Optimized Geometries of Helical Polymers by Using Screw Axis of Symmetry within MNDO Electronic Band Structure Theory

polym	bond length, Å	α,[a] deg	τ,[b] deg	θ,[c] deg	ΔH_f, kcal/mol
$(S)_x$	1.917	108.6	84.4	106.0	-1.90
$(Se)_x$[d]	2.373[e]	106.6	85.8	108.0	
$(CH_2)_x$					
A[f]	1.543 (C-C)	114.0 (CCC)	180.0 (CCCC)	180.0	-4.71
B[f]	1.543 (C-C)	117.3	81.2	99.3	-3.88
C[f]	1.542 (C-C)	118.6	66.5	88.6	-3.88
$(CH_2O)_x$	1.403 (C-O)	123.1 (COC)	81.5	200.6	-41.91
		108.8 (OCO)	82.6		
$(CH_2S)_x$	1.736 (C-S)	114.4 (CSC)	75.7	198.3	-3.72
		109.3 (SCS)	78.1		

[a] Bond angle. [b] Dihedral angle. [c] Helical angle. [d] EHT. [e] Not optimized. [f] See Figure 2.

Proceeding along the lines of the standard self-consistent field linear combinations of atomic orbitals Hartree–Fock (SCF-LCAO HF) approach, the crystal orbitals are expressed as linear combinations of B_p's:[15-17,26]

$$\psi_n(\mathbf{k}) = \sum_p C_{np} B_p(\mathbf{k}) \tag{3}$$

one can obtain the usual **k**-dependent eigenvalue problem[15-17]

$$\mathbf{F(k)\ C(k) = E(k)\ S(k)\ C(k)} \tag{4}$$

where the **k**-dependent Fock matrix **F(k)** is defined by

$$\mathbf{F(k)} = \sum_l \exp(i\mathbf{k}lh)\mathbf{F}(l) \tag{5}$$

and similarly for **S(k)**. The details of the direct space Fock matrices, **F(k)**, have been described by Dewar in the MNDO case elsewhere[21] and are not given here. We note that in calculating all one- and two-electron integrals one has to take the screw symmetry into account by rotating the atomic orbitals relative to a fixed Cartesian coordinate system, i.e., the basis set is the set of the rotated χ^p_l functions. If we choose the screw axis of the helix in such a way that it coincides with the Z axis, the s, p_z and d_{z^2} type orbitals are invariant under the screw operation. The other orbitals can be obtained from the Cartesian orbitals by the relations given in (6), where θ is equal to $2\pi q$, and l labels the lth repeat unit. (Rotated orbitals are in italics.)

$$\begin{aligned}
p_x(l) &= \mathrm{p}_x(l)\cos(\theta l) + \mathrm{p}_y(l)\sin(\theta l)\\
p_y(l) &= -\mathrm{p}_x(l)\sin(\theta l) + \mathrm{p}_y(l)\cos(\theta l)\\
d_{xy}(l) &= -\mathrm{d}_{x^2-y^2}(l)\sin(2\theta l) + \mathrm{d}_{xy}(l)\cos(2\theta l)\\
d_{x^2-y^2}(l) &= \mathrm{d}_{x^2-y^2}(l)\cos(2\theta l) + \mathrm{d}_{xy}(l)\sin(2\theta l)\\
d_{xz}(l) &= \mathrm{d}_{xz}(l)\cos(\theta l) + \mathrm{d}_{yz}(l)\sin(\theta l)\\
d_{yz}(l) &= -\mathrm{d}_{xz}(l)\sin(\theta l) + \mathrm{d}_{yz}(l)\cos(\theta l)
\end{aligned} \tag{6}$$

The extended Hückel parameters used in this paper are taken from ref 27–29 and 40.

Computation of Energetics of Helical Polymers

The geometries of helical systems can be described by parameter sets formed by either bond lengths, bond angles, and dihedral angles or helical radii, the translation along helical axis, and the helical angle.[30-32] For infinite helical chains of the type $(-M_1-M_2---M_n-)_x$, n parameter sets are necessary to define the structure, where M represents the atoms on the backbone chain of the polymer in question. In this paper the former parameter set is used because chemists are more comfortable with bond lengths, bond angles, and dihedral angles. The relationship between the two parameter sets has been established by Shimanouchi.[33] The corresponding computer code we used, which is based on ref 32, was obtained from Dr. A. Karpfen.[34]

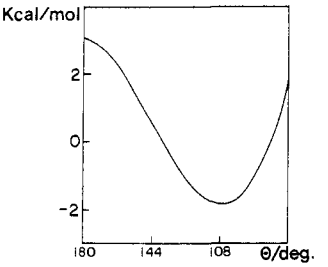

Figure 1. MNDO torsional potential of a sulfur chain (all geometrical parameters are optimized).

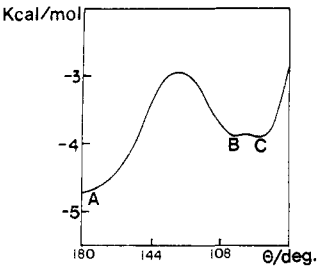

Figure 2. MNDO torsional potential of polyethylene (all geometrical parameters are optimized; A, B, and C are discussed in the text).

We have carried out a full geometry optimization for all systems listed in Table I, except for Se, using MNDO band theory as modified by us for helical systems. Since there are no MNDO[14b] parameters for selenium, the geometry of the selenium chain is optimized at a fixed bond length of 2.373 Å by using the extended Hückel approach. The optimized polymer geometries and the corresponding heats of formation per repeat formula unit are summarized in Table II.

We first review the results and defer the interpretation to the next section. The energy surface for polymeric sulfur has been reported by Springborg and Jones[11r] as well as by Karpfen.[11s] Springborg and Jones have found two minima on the energy surface using a density functional method, but Karpfen has found only one minimum based on ab initio calculation using a large basis set. We have also found one minimum on this energy surface using the MNDO Hamiltonian. Figure 1 shows the torsional potential of helical sulfur, which is in close agreement with Karpfen's potential curve. At the minimum the S–S bond length is shorter than the experimental value by 0.15 Å. The MNDO method usually underestimates the S–S bond distances.[35] The optimized bond angle and dihedral angle are close to the experimental values. The calculated torsional potential barrier (5.66 kcal/mol) is comparable to the value of 8.3 kcal/mol predicted by ab initio calculations.[11s]

(26) Andrê, J.-M.; Vercauteren, D. P.; Bodart, V. P.; Fripiat, J. G. *J. Comput. Chem.* **1984**, *5*, 535.
(27) Hughbanks, T.; Hoffmann, R.; Whangbo, M.-H.; Stewart, K. R.; Eisenstein, O.; Canadell, E. *J. Am. Chem. Soc.* **1982**, *104*, 3876.
(28) Whangbo, M.-H. *Solid State Commun.* **1982**, *43*, 637.
(29) Zheng, C.; Hoffmann, R.; Nesper, R.; Schnering, H. G. v. *J. Am. Chem. Soc.* **1986**, *108*, 1876.
(30) Miyazawa, T. *J. Polym. Sci.* **1961**, *39*, 746.
(31) Sugeta, H.; Miyazawa, T. *Biopolymers* **1967**, *5*, 673.
(32) Yokouchi, M.; Tadokoro, H.; Chatni, Y. *Macromolecules* **1974**, *7*, 769.
(33) Shimanouchi, T.; Mizushima, S. *J. Chem. Phys.* **1955**, *23*, 707.
(34) Karpfen, A., private communication, 1988.
(35) (a) Baird, N. C. *J. Comput. Chem.* **1984**, *5*, 35. (b) Dewar, M. J. S.; McKee, M. L. *J. Comput. Chem.* **1983**, *4*, 84.

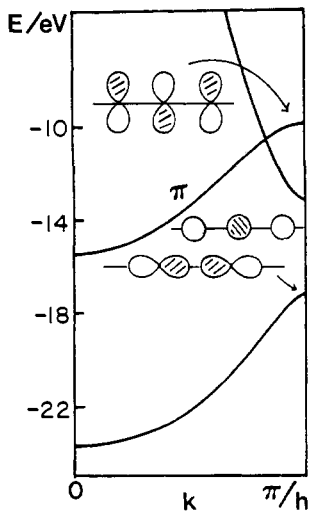

Figure 3. EHT band structure of linear sulfur chain.

The computed geometry of the selenium chain is only in qualitative agreement with the experimental structure. This can be traced back to the stronger interchain interactions between selenium chains.[36] The calculated interchain and intrachain overlap populations are 0.237 and 1.285, respectively, based on a full three-dimensional EHT calculation on trigonal selenium. Thus, isolated chain geometry can be only qualitatively compared with the experimental structure.

For polyethylene we have located three local minima on the energy surface. Figure 2 shows the torsional potential of polyethylene. The energy values on the figure correspond to fully relaxed geometries at a fixed value of θ. The lowest minimum corresponds to an all-trans structure (A in Figure 2) and two others (B and C) to gauche conformations. The differences in energy between *all-trans*- and *gauche*-polyethylene is 0.83 kcal/mol, which is close to the value of 0.87 kcal/mol as calculated by ab initio calculation without full geometry optimization.[11a] Similar results have been obtained by means of the EHT method.[11p]

MNDO calculations correctly predict that poly(oxymethylene) exists in a gauche conformation. The calculated helical angle of 200.6° is close to the experimental value of 198.6°.[9b] This result is better than the value of 188.7° calculated by an initio calculation without full geometry optimization.[11u] Poly(thiomethylene) is calculated to be preferably in a gauche conformation as well. The available experimental information on poly(thiomethylene) structure is limited. Its helical angle is 190.6°,[9c] which should be compared with the calculated value of 198.0°.

As a general trend, Table II shows that the polymers with a gauche conformation have a bond angle of about 100° and a dihedral angle of about 80°, indicating a qualitatively similar arrangement of the main-chain atoms. What factors make these polymers accept such common geometries and the reason the torsional potential curves for sulfur chain and polyethylene as shown in Figures 1 and 2 are remarkably different are the subject of the next two sections.

Discussion

Polymeric Sulfur and Selenium. Let us begin with a linear sulfur chain, which is obviously a high-energy conformation. The band structure calculated by means of the extended Hückel approximation is shown in Figure 3 using the experimental sulfur–sulfur bond length. The band that lies lowest in energy is a sulfur–sulfur bonding band which can be considered to be generated by localized sulfur–sulfur bonding orbitals formed by two sp hybrid orbitals on adjacent atoms. The two degenerate π bands are generated by $3p_x$ and $3p_y$ orbitals from each atom. The band lying highest in energy is sulfur–sulfur antibonding. Figure 3 shows the crossing

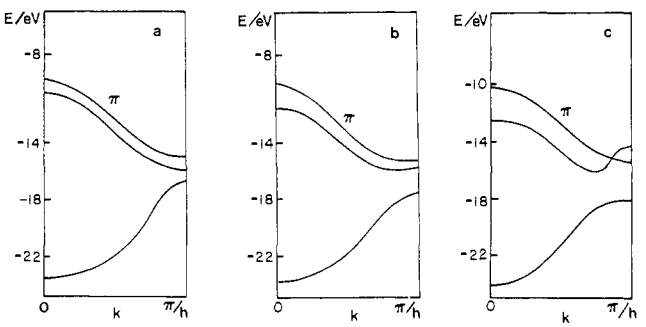

Figure 4. EHT band structures of zigzag planar sulfur chains with bond angles of 150° (a), 120° (b), and 99.2° (c). (Only occupied bonds are given.)

of the π bands and this σ band. The nodal structures of the crystal orbitals at the edge of the Brillouin zone (BZ) shown in Figure 3 illustrate this point. Therefore, a linear sulfur chain has partially filled bands. Peierls' theorem tells us that such a system is unstable and will undergo such geometry distortions that allow lowering of the total energy by a geometrical rearrangement so as to open a gap between the highest occupied and lowest empty levels (E_g).[37] If the partial filling of a band is the ratio of small integers n/m, one such mode is easily identified: the unit cell will m-merize to open a gap. For example, the bond-length alternation of polyacetylene[10] or the clustering in partially charged iodine[38] or Hg chains[39] can be easily understood. For linear sulfur the partial filling occurs at a general point in the Brillouin zone. Therefore, we pursue a different line of argument. Because two π bands are almost completely filled, the linear sulfur chain gets an overall destabilization from π electrons. This situation results from the well-known four-electron repulsion.[24,40] A way to stabilize such a chain is to decrease π-electron repulsions, which can be achieved by allowing a zigzag conformation to form as shown in **3**. As

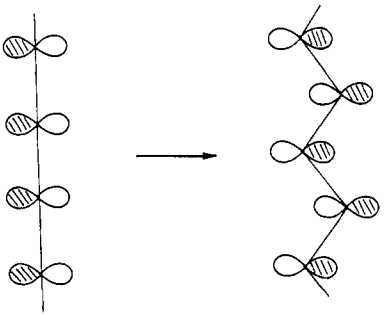

3

the bond angle, α, starts to decrease from 180°, the symmetry of the chain changes abruptly: Bloch functions formed from the s and p_z function remain unchanged but for p_x and p_y, as discussed in the section on calculational methods, the Bloch functions become pseudo-Bloch functions, corresponding to a different **k** point owing to the fact that the screw operation changes the phase of such orbitals. Consequently, the band structure for $\alpha \rightarrow 180°$ (but $\alpha \neq 180°$) has a π band that is the mirror image of the one for the $\alpha = 180°$ (linear) chain (see Figure 4a). As α is decreased from 180°, the in-phase π band becomes of σ symmetry and starts to mix with the other σ bands. First, it splits off from the π band, as illustrated for $\alpha = 150°$ in Figure 4b. A further decrease ($\alpha = 120°$) shows that as the bond angle further decreases, toward the end of the BZ the σ bands start to repel one another due to an avoided crossing (Figure 4c). At the optimized geometry ($\alpha = 99.2°$, Figure 4c) this repulsion leads to a crossing of the π and σ bands near $\mathbf{k} = \pi/h$. The optimized bond angle for the selenium

(36) Joannopoulos, J. O.; Schluter, M. A.; Cohen, M. L. In *Proceedings of the Twelfth International Conference on the Physics of Semiconductors (Stuttgart)*; Pilkun, M. H., Ed.; Teubner: Stuttgart, 1974.

(37) Peierls, R. E. *Quantum Theory of Solid*; Oxford University Press: London, 1955.

(38) Kertesz, M.; Vondervisztt, F. *J. Am. Chem. Soc.* **1982**, *104*, 5889.

(39) Kertesz, M.; Guloy, A. M. *Inorg. Chem.* **1987**, *26*, 2852.

(40) Burdett, J. K. *Molecular Shapes*; Wiley: New York, 1980.

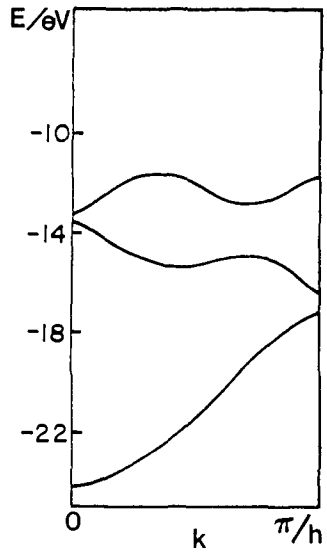

Figure 5. EHT band structure (occupied bands) of gauche polymeric sulfur with MNDO optimized geometry.

chain is 102.4° by using the extended Hückel approach and a fixed bond length of 2.373 Å, and for the sulfur chain the optimized bond angle is 99.2° as obtained for a fully optimized all-trans conformation by the MNDO approach. Both values are in agreement with our qualitative analysis. The band structures for an all-trans sulfur chain corresponding to the bond angle of 99.2° are shown in Figure 4. It can be seen that the p_y (π) band is unchanged in energy. The band width for the σ band, derived from the p_x orbitals, which are of π symmetry for the linear chain, is decreased by 2.0 eV, indicating that the closed-shell repulsions associated with this p_x (σ) derived band are smaller than for a linear chain. The formation of the zigzag chain adds 1.5 eV (EHT) to the stability of the sulfur chain. The general relationship between energetics of closed-shell repulsion and band width (BW) is given in the Appendix.

Similarly, we can minimize the repulsions among the π electrons in the p_y band by reducing the dihedral angle of 180° for all-trans sulfur to about 90° as illustrated in **4**. The optimized dihedral

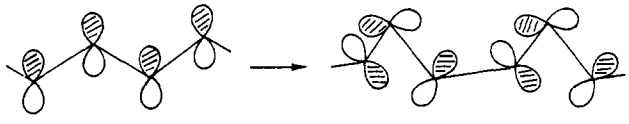

4

angle is 85.8° for selenium chain and 84.4° for sulfur chain. In this case the mirror plane is lost, and no bands can cross. The band structure for a gauche sulfur chain with the optimized dihedral angle is presented in Figure 5, which is in agreement with that calculated by the ab initio crystal method using a large basis set;[11s] the one for selenium is given in Figure 6. It can be seen from Figure 5 that the width of the band originated from the p_y band in the planar case becomes very narrow. In other words, the closed-shell repulsion is effectively reduced between electrons in p_y orbitals, just like we saw it for the p_x orbitals. The sulfur–sulfur bond is also strengthened by the mixing of the p_y band and the sulfur–sulfur bonding bands at the same time. This mixing increases the sulfur–sulfur overlap populations from 0.567 to 0.609 (EHT values). The formation of the helix leads to a further stabilization by 0.25 eV for selenium chain and by 0.33 eV for sulfur chain relative to the zigzag conformation.

It should be pointed out here that the valence-shell electron-pair repulsion (VSEPR) theory[41] would predict that for the polymeric sulfur both all-trans and gauche (G_4, where the bond angle is

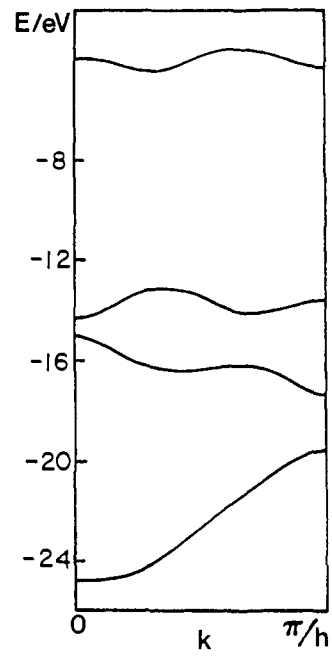

Figure 6. EHT band structure of gauche selenium chain with EHT optimized geometry. (The lowest three are occupied.)

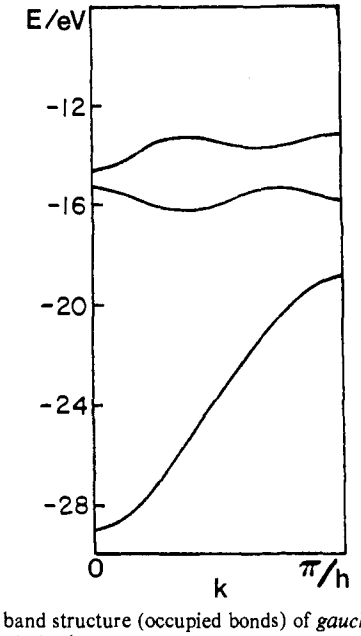

Figure 7. EHT band structure (occupied bonds) of *gauche*-polyethylene with MNDO optimized geometry.

109.5° and dihedral angle is 60.0°) would be stable conformations. The analysis of orbital interactions is necessary to predict which of the two conformations are energetically more favorable. Another such example has been given by Burdett for the case of elemental phosphorous.[42] The above analysis for polymeric sulfur gives a handle on more complex cases as discussed in the subsequent section.

Polyethylene and Polysilane. For polyethylene, $(CH_2)_x$, the situation becomes somewhat more complex by the addition of two H(1s) orbitals as compared to polymeric sulfur and selenium. Figure 7 shows band structures for *gauche*-polyethylene with a helical angle of 99.3°. Comparison of Figure 7 with Figures 6 and 5 shows that band structure for *gauche*-polyethylene is quite similar to that of gauche sulfur and selenium chains. One can conclude that similar factors govern the geometries of these polymers and the orbital interaction schemes in these three

(41) Gillespie, R. J. *Molecular Geometry*; Van Nostrand Rheinhold: London, 1972.

(42) Burdett, J. K.; McLarnan, T. J. *J. Chem. Phys.* **1981**, *75*, 5764.

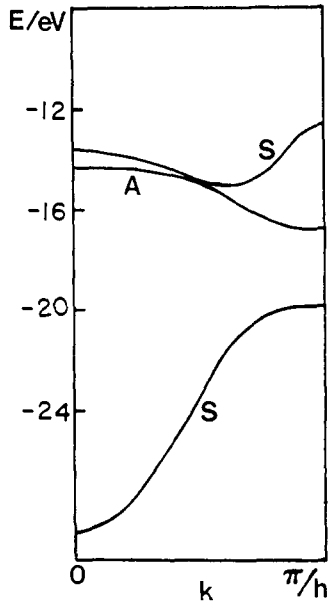

Figure 8. EHT band structure of *all-trans*-polyethylene (A and S are antisymmetric and symmetric with respect to polymer plane, respectively).

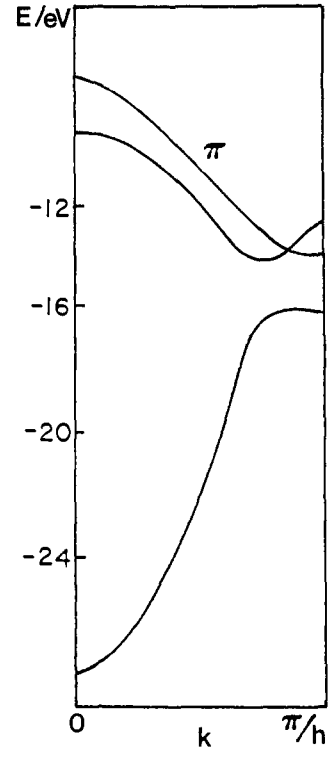

Figure 9. EHT band structure of all-trans model carbon chain obtained by omitting all protons from polyethylene.

polymers are remarkably similar since the directions to which the C–H bonding electron pairs point are similar to those of the lone electron pairs on sulfur atoms of gauche polymeric sulfur.

Let us progress to the question of why *all-trans*-polyethylene is stable as well. As we have shown above, the instability of the all-trans sulfur chain comes from the fully filled π band formed by p_y orbitals. In the case of *all-trans*-polyethylene, however, the same p_y orbitals are used for C–H bonding rather than for a π band. This weakens the interactions between electrons in the p_y orbitals on adjacent atoms substantially. The narrow band which is antisymmetric with respect to the polymer plane (A in Figure 8) confirms this point and indicates the weak closed-shell repulsions between C–H bonds. Quite similar band structure has been reported based on ab initio calculations.[26] Thus, the driving force

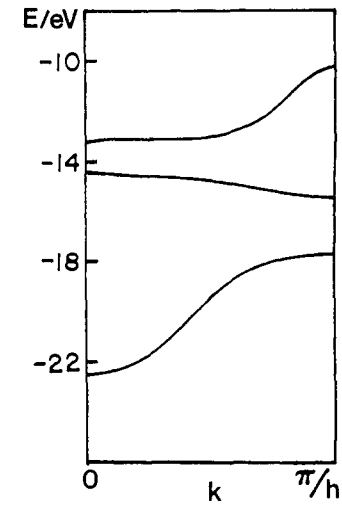

Figure 10. EHT band structure of *all-trans*-polysilane.

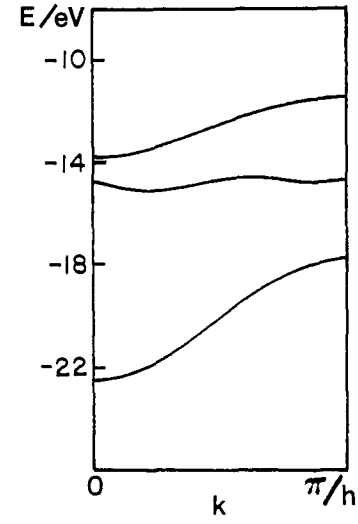

Figure 11. EHT band structure of *gauche*-polysilane.

pushing the all-trans sulfur chain toward a gauche conformation is much weakened or absent in $(CH_2)_x$. This explains why *all-trans*-polyethylene is also one of the energetically favorable conformations. To understand further what role hydrogen atoms play in *all-trans*-polyethylene, we show in Figure 9 the band structure of a zigzag carbon chain obtained by omitting all protons from *all-trans*-polyethylene. The most important difference between Figure 9 and Figure 8 from the point of view of the stabilities of planar vs. gauche configurations is that the width of the second highest occupied valence band for *all-trans*-polyethylene, which is the π band (antisymmetric with respect to the polymer plane), is narrower than that for the carbon chain by 4.7 eV (see the Appendix for the relationship of closed-shell repulsion and the band width). Attaching the two protons per carbon to the carbon chain dramatically reduces the repulsions between the π electrons. As a result, polyethylene has a minimum on the energy surface at a helical angle of 180°.

Based on the analysis of factors influencing the geometry of polyethylene, one could predict that polysilane would have two stable conformations: all-trans and a gauche. Figures 10 and 11 show the band structures of all-trans and gauche conformations of polysilane with standard bond length (2.342 Å) bond angle (109.47°), and dihedral angles (180.0° and 60.0°), respectively.[1a] The band structure of *all-trans*-polysilane is different from that of $(CH_2)_x$ in the way that the highest and next highest occupied bands are separated owing to the low ionization potential of the p orbital of silicon atom. Most of the previously calculated band structures of *all-trans*-polysilane are in general agreement with our results.[43] Polysilane is considered to be more flexible than

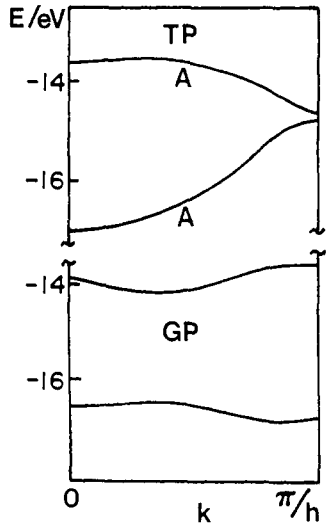

Figure 12. EHT π occupied band structures that are antisymmetric with respect to the plane of poly(oxymethylene) (TP) and the corresponding two bands for *gauche*-poly(oxymethylene) (GP).

polyethylene.[44] Our EHT calculations show that *gauche*-polysilane is slightly more stable than the all-trans one. A mixture of trans and gauche conformations might explain the experimental UPS and XPS results,[45] similar to the case of polyethylene.[46]

Poly(oxymethylene) and Poly(thiomethylene). Usually, conformations are governed by intramolecular interactions that include (a) potential energy hindering the internal rotation around a single bond, (b) repulsive forces and van der Waals attractions between nonbonded atoms or groups, (c) electrostatic interaction, and (d) hydrogen bonding.[1b] If only interactions a and b are taken into account, the planar zigzag and the G_4 helix (bond angle 109.47° and dihedral angle 60°) are considered to be stable for poly(oxymethylene) and poly(thiomethylene) as shown in **5**. Tadokoro's

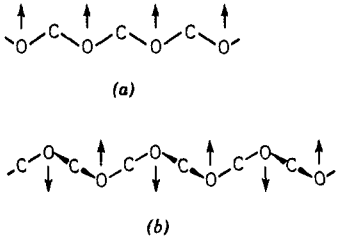

5

explanations of why the latter conformation is more stable than the former emphasize that in the zigzag conformation the dipole moment vectors produced by the COC groups are parallel which is unfavorable in comparison with the alternating antiparallel arrangements of the helical conformation.[47] In fact, for both polymers with a zigzag conformation there are two bands which corresponds to the π band of zigzag polymeric sulfur as shown in Figure 12. The electrons in the two bands give rise to destabilizing closed-shell repulsions, just like the π electrons in the case of planar zigzag polymeric sulfur. As a result, the polymer tends to decrease the dihedral angle in order to reduce these repulsions. Figure 12 shows the corresponding bands which are very flat for the polymer with the optimized gauche geometry.

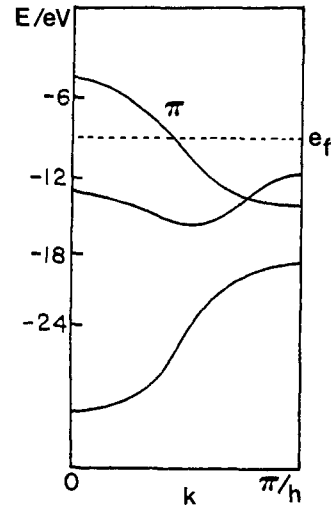

Figure 13. EHT band structure of polyacetylene (C–C = 1.40 Å, C–H = 1.10 Å, all bond angles are 120°, all C–C bonds are equivalent). e_f indicates the Fermi level.

Changing the Electron Counting: Polyacetylene, Li_2Ga, and Crystals with CrB Structure. If one electron is taken out from every sulfur atom of zigzag polymeric sulfur, the resulting chain is isoelectronic with polyacetylene, $(CH)_x$.[10] Because the electrons we removed in this process occupy the π-antibonding crystal orbitals, the driving forces toward the polymeric sulfur screw are removed, and a delocalized π band for sulfur–sulfur bonding is produced. For $(S^+)_x$, the EHT calculations show that the planar zigzag structure is more stable than the gauche one by 0.38 eV, using the rigid band model (see Figures 4 and 5). Actually, any distortion from the planar zigzag structure will lead to loss of π bonding and thus increase the energy of the system. The MNDO optimization on the structure of a nitrogen chain $(N)_x$, which is isoelectronic with $(S^+)_x$, shows that the minimum energy corresponds to a planar zigzag structure with a bond length alternation of 1.238 and 1.382 Å. For comparison, the standard N–N single- and double-bond distances are 1.46 and 1.23 Å.[1a] One can expect that the band dispersions for polyacetylene are similar to that of zigzag sulfur chain, and this is indeed the case as shown in Figure 13 for $(CH)_x$. (The equidistant polyacetylene model just as $(N)_x$ has an odd number of electrons in the repeat unit and therefore has a half-filled band, the bond-length alternation will be induced by a Peierls distortion.[10,37] Our point in discussing polyacetylene here is merely to show that the same orbital picture that predicts polymeric sulfur to be gauche also predicts that polyacetylene should be planar.)

A somewhat similar situation occurs for the Ga chains (**6**) in

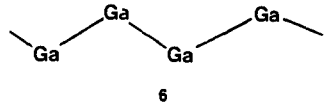

6

Li_2Ga.[5b] We have performed a three-dimensional EHT band calculation on this compound, which indicates that there should be an appreciable amount of charge transferred from Li to Ga (the gross atomic charges are −1.10 and +0.55 on Ga and Li atoms, respectively). Even though the difference in electronegativity between Li and Ga is small, a substantial charge transfer is favored because of the lower lying Ga–Ga bonding levels made available by the formation of the Ga chains. The calculated Ga–Ga and Ga–Li overlap populations in Li_2Ga are 0.82 and 0.16, respectively, indicating strong Ga–Ga and much weaker Ga–Li bonding. In agreement with the bonding picture in which there is some π bonding between Ga atoms in the Ga chain in addition to σ bonding, the observed Ga–Ga distance in Li_2Ga is 2.62 Å, which is much smaller than twice the metallic radius (3.06 Å).[1a]

There is a large group of binary borides that contain zigzag planar trans boron chains. Several known examples of such crystals are FeB, MoB, NbB, TaB, VB, CoB, MnB, TiB, HfB,

(43) (a) Dyachkov, P. N.; Ioslovich, N. V.; Levin, A. A. *Theor. Chim. Acta* **1975**, *40*, 237. (b) Takeda, K.; Matsumoto, N.; Fukuchi, M. *Phys. Rev.* **1984**, *B30*, 5871. (c) Takeda, K.; Matsumoto, N. *J. Phys.* **1985**, *C18*, 6121. (d) Teramae, H.; Yamabe, T.; Imamura, A. *Theor. Chim. Acta* **1983**, *64*, 1.
(44) Damewood, J. R., Jr.; West, R. *Macromolecules* **1985**, *18*, 159.
(45) Bock, H.; Ensslin, W.; Feher, F.; Freund, R. *J. Am. Chem. Soc.* **1976**, *98*, 668.
(46) Kertesz, M.; Göndör, G. *J. Phys.* **1981**, *C14*, L851.
(47) Tadokoro, H. *Kobunshi No Kozo* (in Japanese); Kagakudojin: Kyoto, 1976.

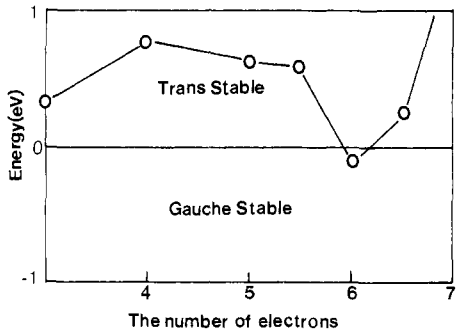

Figure 14. Relative stability of all-trans and gauche boron chains as a function of the number of valence electrons per boron (B–B = 1.77 Å, for all-trans structures all bond angles are 120°, for gauche structure all bond angles are 109.47°, and dihedral angle = 60°).

WB, and NiB.[5a,c-m] For example, in the CrB structure there are zigzag chains of boron atoms with a uniform boron–boron bond distance of 1.72 Å,[5a] and in the similar FeB this value is 1.77 Å,[5c] corresponding to covalent boron–boron bond distances. Three-dimensional EHT calculation on CrB shows that B–B and B–Cr overlap populations are 0.52 and 0.21, respectively. The large B–B overlap population indicates that B–B bonding plays a very important role in determining the conformation of the boron chain although there is significant interaction between boron chains and Cr atoms. The following calculations illustrate the role of energetics of an isolated boron chain in determining whether it assumes a gauche or all-trans conformation. Figure 14 shows EHT energy band calculations of the stability of the zigzag form of boron chain relative to the gauche form as a function of the number of valence electrons. It can be seen that within the range of the number of electrons from somewhat less than three to little smaller than six the all-trans structure is more stable. It seems, therefore, that there is no electronic driving force toward a screw in these materials for any conceivable electron counting. Due to the appreciable metal–boron bonding in these structures a direct comparison of the isolated chain result with experiment is not possible; it is satisfactory to note that all such structures exhibit a planar zigzag boron "chain".

Another group of binary compounds MA (M = Ca, Sr, Ba; A = Si, Ge, Sn, Pb) also has the CrB structure, in which the A atoms form zigzag chains. The A atom chains (group IVA) would be isoelectronic with the sulfur chain if the atom A obtained two electrons from the metal atom M. This is a good assumption only when A atom is a strong electron acceptor such as Cl and O. In our cases, however, this is unrealistic because main-group IVA atoms are not strong enough electron acceptors. We have performed three-dimensional EHT calculations for CaSi and found that each Ca atom offers approximately 1.20 electrons (Mulliken population value) to each Si atom. Therefore, the main atom chains in this group of binary compounds lie in the region of Figure 14 where trans conformation is expected to be more stable.

The effect of the ability of metal atoms to offer electrons on conformation is easily visualized by comparison of $CaSb_2$[7e] (**7**)

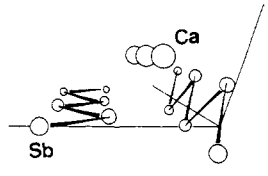

7

and CsSb[7] phases. The CsSb phase has the NaP structure (**8**) and the Sb atoms form distorted 4-fold helical chains. Similar chains in $CaSb_2$, however, form the zigzag structure **7**. Concerning the number of electrons transferred from the M metal atoms to the Sb atoms, it appears that the two Cs atoms per two Sb offer more electrons than one Ca atom, consistent with the fact that the second ionization energy of Ca (11.87 eV) is much higher than the first ionization energy of Cs (3.78 eV).[48]

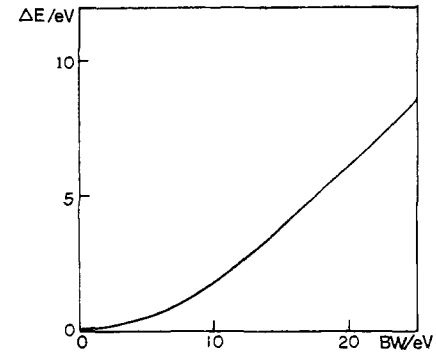

Figure 15. Destabilization energy (ΔE) of an $(H^-)_x$ chain as a function of the band width (BW).

Crystals with NaP Structure. The crystals that exist in the NaP structure **8** or in closely related structures are AM (M = Li, Na,

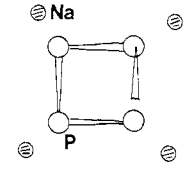

8

K, Rb, Cs; A = P, As, Sb).[7] The NaP structure is characterized by the existence of a distorted 4-fold helical P atom chain. Owing to the lower ionization potential of sodium, the P atom chain is better described as $(P^-)_x$, which is isoelectronic with the sulfur chain. Apparently, the structures of the main-group atomic chains of these phases can be also understood by using the conclusions obtained from the conformation analysis of the sulfur chain.

Conclusions

In this work we conclude that the electron repulsions that come from the occupation of antibonding crystal orbitals are responsible for the helical conformation of many main-group polymers which range from typical organic polymers such as poly(oxymethylene) and polyethylene to standard inorganic polymers such as polymeric sulfur and phosphorus atomic chains in NaP (see also the Appendix). The studies of the effect of changing electron counting on the conformation of helical polymers show that an all-trans conformation for the polymers with the number of valence electrons in the repeat unit significantly different from six is energetically favorable, while the polymers having close to six valence electrons in the repeat unit are more likely to be in the gauche conformation as shown in Figure 14. The stability of the all-trans conformation of polyethylene and polysilane results from the absence of π-electron repulsions by the formation of C–H and Si–H bonds. Another conclusion is that the geometry of helical polymers predicted by the MNDO crystal orbital approach is in good overall agreement with experimental observations.

Acknowledgment. This work was supported by the National Science Foundation through Grant DMR-8702148 and the Camille and Henry Dreyfus Foundation (1984–1989). We are indebted to Dr. A. Karpfen for allowing us to use his program that produces helical coordinates from internal coordinates. We thank an anonymous referee for prompting us to establish the quantitative relationship between band width and closed-shell repulsion presented in the Appendix.

Appendix

The closed-shell repulsions in an infinite chain that we have discussed in the text are due to the fact that antibonding and bonding π crystal orbitals are both occupied, which in turn is related to the width of the energy band. Below is an attempt to

(48) *Handbook of Chemistry and Physics*, 69rd ed.; Chemical Rubber Co.: Cleveland, 1988; p E78.

correlate this effect with the corresponding band width (BW). In the first-nearest-neighbor's approximation, the π-energy band of the zigzag planar sulfur chain in the framework of the EHT is

$$E(\mathbf{k}) = \frac{H + 2KSH\cos(\mathbf{ka})}{1 + 2S\cos(\mathbf{ka})} \quad (7)$$

where $\mathbf{k}$ is the wave vector, S is the overlap integral, H is the valence-state ionization potential of the p_z orbital, $\mathbf{a}$ is the lattice spacing, and K is the Wolfsberg-Helmholtz constant. The π-energy loss due to closed-shell repulsion in an energy band per repeat unit can be approximated by averaging over two $\mathbf{k}$ points ($\mathbf{k} = 0.0$ and $\pi/\mathbf{a}$), and is given up to second order in overlap by

$$\Delta E \approx -16HS^2 \quad (8)$$

where $K = 2.0$. The corresponding BW is approximately given by

$$\mathrm{BW} \approx |4HS| \quad (9)$$

Because S^2 is greater than 0 and H is less than 0, the smaller the S, the smaller the repulsion. Thus, the narrower the band, the weaker the electron repulsions, and the relationship is approximately quadratic ($\Delta E \approx -(\mathrm{BW})^2/H$). In the case of polymeric sulfur, the polymer is forming a screw conformation to make the $3p_z$ orbitals almost orthogonal ($S \approx 0.0$). As an illustration, Figure 15 shows the averaged energy of the $(H^-)_x$ chain per H atom relative to the situation of no closed-shell repulsions as a function of the BW on the basis of the extended Hückel solid-state calculation (six $\mathbf{k}$ points). The energy loss due to closed-shell repulsion is approximately quadratic in the BW up to 10-15 eV.

The Gas-Phase Smiles Rearrangement: A Heavy Atom Labeling Study

Peter C. H. Eichinger,[1a] John H. Bowie,*[1a] and Roger N. Hayes[1b]

Contribution from the Department of Organic Chemistry, University of Adelaide, Adelaide, South Australia, 5001, Australia, and Department of Chemistry, University of Nebraska, Lincoln, Nebraska 68588-0362. *Received September 19, 1988*

Abstract: Heavy atom (^{13}C and ^{18}O) labeling shows that the product ion PhO^- from $PhO(CH_2)_2O^-$ and products PhO^- and PhS^- from $PhS(CH_2)_2O^-$ are formed through Smiles intermediates I (X = Y = O or X = O, Y = S). The analogous product

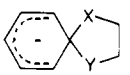

I

ions from $PhO(CH_2)_3O^-$ and $PhS(CH_2)_3O^-$ are formed by two processes. It is likely that these are (i) Smiles and (ii) S_Ni attack by O^- at the methylene group $PhXCH_2$. The extent of the Smiles process decreases as n increases for systems $PhX(CH_2)_nO^-$. The Smiles rearrangement does not occur for ions $PhO(CH_2)_nS^-$ (n = 2-6).

The classical (condensed phase) Smiles rearrangement[2] is summarized in eq 1. The nucleophilic attack normally requires an electron-withdrawing group (e.g., nitro, sulfonyl, or halogen) either in the ortho or para position on the aromatic ring; generally X is a good leaving group, and Y is a strong nucleophile.[3]

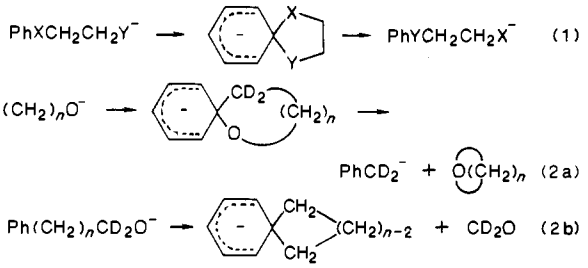

Collisional activation of ions $PhCD_2(CH_2)_nO^-$ (n = 2-4) in the gas phase result in the formation of $PhCD_2^-$.[4] The possibility of a Smiles rearrangement (eq 2a) was suggested although S_Ni attack at the β carbon (β to phenyl) could not be excluded. Similarly, ions $Ph(CH_2)_nCD_2O^-$ (n = 2 and 3) eliminate CD_2O, and a Smiles product ion (eq 2b) was proposed.[5] We were not able to substantiate the mechanistic proposals shown in eq 2a and 2b, but if they are correct it means that gas-phase Smiles rearrangements do not require the activation of the benzene ring by an ortho or para electron-withdrawing group.

In this paper we report a study of gas-phase systems where the operation of Smiles rearrangements can be tested experimentally. We report the operation of gas-phase Smiles rearrangements for species related to those shown in eq 1, in particular when X = Y = O and when X = S and Y = O. The mechanisms are substantiated by heavy atom (^{13}C, ^{18}O) labeling studies.

Experimental Section

Collisional activation mass spectra (MS/MS) were recorded with a Vacuum Generators ZAB 2HF mass spectrometer operating in the negative chemical ionization mode.[6] All slits were fully open to obtain maximum sensitivity and to minimize energy resolution effects.[7] The chemical ionization slit was used in the ion source, ionizing energy 70 eV (tungsten filament); ion source temperature 150 °C; accelerating voltage -8 kV. Deprotonation of the appropriate neutral substrate was effected by HO^- (or H^- or $O^{\cdot-}$). Reactant negative ions were generated from water with 70 eV electrons.[8] The indicated source pressure of H_2O was

(1) (a) Adelaide. (b) Lincoln.
(2) Warren, L. A.; Smiles, S. *J. Chem. Soc.* **1930**, 956 and 1327.
(3) For a review, see: Truce, W. E.; Kreider, E. M.; Brand, W. W. *Organic Reactions*; John Wiley and Sons: New York, 1970; Vol. 18, pp 99. See, also: Schmidt, D. M.; Bonvicino, G. E. *J. Org. Chem.* **1984**, *49*, 1664 and references cited therein.
(4) Raftery, M. J.; Bowie, J. H.; Sheldon, J. C. *J. Chem. Soc., Perkin Trans. 2* **1988**, 563.
(5) Similar ions have been proposed as intermediates in solution reactions, see: Staley, S. W.; Cramer, G. M.; Kingsley, W. G. *J. Am. Chem. Soc.* **1973**, *95*, 5052. Bertrand, J. A.; Grovenstein, E.; Lu, P.-C.; Vanderveer, D. *J. Am. Chem. Soc.* **1976**, *98*, 7835.
(6) Terlouw, J. K.; Burgers, P. C.; Hommes, H. *Org. Mass Spectrom.* **1979**, *14*, 307.
(7) Burgers, P. C.; Holmes, J. L.; Mommers, A. A. Szulejko, J. *J. Am. Chem. Soc.* **1984**, *106*, 521.

0002-7863/89/1511-4224$01.50/0